Chapter IV

Microbial binding: controlling factor of slope angles in post-Triassic carbonate slopes?

Abstract

The geometry and inclination of carbonate platform slopes are tipically described as the result of the sediment texture, components, and grain size occurring in the slope. Three carbonate slopes from the Holocene of the Tongue of the Ocean (Bahamas) and three slopes from an Upper Miocene carbonate platform in SE Spain were selected to identify the factors controlling dip angles. Although platforms differ in size and elevation with regard to the surrounding basin, both locations present slopes with linear profiles and steep angles over 35°. Petrographic analysis shows that the slope facies in both locations are similar with the matrix and some bioclasts presenting microfabrics indicative of the presence of microbial activity during deposition. These include (1) clotted micrite patches locally connecting bioclasts or infilling primary pores; (2) porostromate structures in the micrite; (3) dense micritic masses; (4) binding structures; (5) micritic envelopes; and (6) peloidal textures. The Holocene and Miocene depositional geometries and facies distribution are the response to different sedimentary processes including rockfalls, gravity flows, and in-situ carbonate production. The presence of an extensive microbial influence is proposed as a controlling factor of slope angles, a stabilizing factor of the steep slope as significant as in Palaeozoic and Triassic examples.

4.1 Introduction

Carbonate platform slopes form the transition between shallow-water shelf carbonates and deep-water basinal deposits, and one that is shaped by a series of different depositional and diagenetic processes. Factors controlling the slope geometry include the volume of sediment exported from the platform and the platform height (Schlager, 1981), the grain size (Kirkby, 1987), the erosion-deposition balance (Schlager and Camber, 1986), the response to shear strengths in fine-grained carbonate slope sediments (Kenter, 1990; Kenter et al., 2005; Schlager, 2005; Playton et al., 2010), early lithification (Grammer et al., 1993a; 1993b), and in-situ carbonate production and stabilization (Kenter, 1990; Della Porta et al., 2003; 2004; Kenter et al., 2005).

Carbonate slopes with angles steeper than 30°-45° in Palaeozoic and Triassic platforms are described as the result of stabilization by organic framebuilding, by microbial binding and by early lithification (Kenter, 1990; Adams and Kenter, 2014; Keim and Schlager, 2001; Della Porta et al., 2003; 2004; Kenter et al., 2005). In such platforms, organic framebuilding and early lithification are more significant than grain size in determining the slope geometry. In post-Triassic examples, Cretaceous of Mexico (Enos, 1977) and Miocene of the Gulf of Suez (Haddad et al., 1984), it was discussed if the steep angles of carbonate slopes are due to early submarine cementation or by sediment binding by various organisms. Microbial stabilization of the slope was recently described as playing a significant role in Neogene (Upper Miocene) carbonate platform slopes of the Mediterranean realm (Reolid et al., 2014). However, those results may be only conditionally accepted, as the platform studied was formed in a satellite basin of the Mediterranean where water circulation was becoming restricted as a prelude of the Messinian Salinity Crisis and the coral reefs grew with "aberrant" features (Esteban, 1980). These features include low reef-building species diversity, ample development of monospecific *Porites* reefs, and the presence and abundance of microbial related deposits, mainly forming stromatolites but also stabilizing *Halimeda* bioherms (Braga et al., 1996; Martín et al., 1997), and *Porites* reefs (Riding et al., 1991). While the presence of thick microbial deposits has been proved to be a common phenomenon in Holocene reef environments of normal marine conditions as the barrier reef of Tahiti (Camoin, 1999), and the Great Barrier Reef (Webb and Jell, 1997); the significance of microbial binding in slope deposits has not yet been determined. In order to test whether microbial stabilization of the slope is a frequent phenomenon in post-Triassic slope deposits, or if it is exclusively present in the especial Miocene Mediterranean outcrops, an example of steep slopes from well known carbonate platforms with normal marine conditions were studied.

Steep slope angles were described from the Tongue of the Ocean in the Bahamas carbonate platform (Grammer, 1991; Grammer and Ginsburg, 1992; Grammer et al., 1993a; 1993b). The origin of the steep angles was originally attributed to early cementation of the slope. Microfacies analysis, however, indicates many similarities to Upper Miocene Mediterranean slope facies, where microbial stabilization is significant. The aim of this study is thus to identify, characterise and quantify the presence of microbial binding in the Holocene slope from the Bahamas, to evaluate the microbial contribution to the slope architecture, and to compare both slope depositional systems, in the Bahamas and Mediterranean domain, for a better understanding of the microbial slope stabilization in post-Triassic deposits. Results indicate that microbial binding occurs throughout the slopes analysed.

4.2 Geological setting

Great Bahama Bank consists of a more than 104.000 km^2 of tropical shallow-water carbonate banks separated by deep troughs (Willian et al., 1989). One of these deep-water troughs is the Tongue of the Ocean (TOTO), which represents an extension of the Atlantic Ocean between the islands of New Providence and Andros (Fig. 4.1A). TOTO is a 1500 to 3600 m deep trough which is 160 km long and 32 to 64 km wide. The bottom of this embayment has a northward-deepening V-shaped profile between Andros and New Providence Islands changing into a U-shaped cul-de-sac in the south, where the studied slopes are located (Fig. 4.1A) (Andrews et al., 1970). These are located at the leeward (Privitt Place slope and Palmer Point slope) and windward flanks (Rock Range slope) of TOTO respectively (Fig. 4.1A). The sedimentary record in the cul-de-sac consists of gravity flow deposits composed of rubble and sand whose components vary according to the distribution of surface sediments on the surrounding platform (Grammer and Ginsburg, 1992). Grainy deposits are frequently intercalated with pelagic lime mud, especially in the lower portions of the slope (Schlager and James, 1978; William et al., 1989).

During the Messinian, the Sorbas Basin in southeast Spain (Fig. 4.1B) was rimmed by tropical carbonate platforms (Martín and Braga, 1994). The studied slopes represent three consecutive progradational stages of the Cariatiz carbonate platform. The present tectonic tilt of this platform is less than 3 degrees (Braga and Martín, 1996).

4.3 Methods

A total of 134 submersible dives with the two-person submersible *Delta* (Delta Oceanographics) were made during 3 cruises from 1988-1990 to characterize the different slopes of the TOTO (Grammer, 1991). Description and measurements of the different

features in the slope were documented by videotape and photography. Slope angles were obtained using a hand-held inclinometer from the inside of the submersible. A total of 90 samples from the three slopes were selected to define the facies and microfacies. Polished slabs and thin sections were made out of the lithified samples. The slope angles and general features presented herein were extracted from Grammer (1991). The petrographical data were obtained from Grammer (1991) and amended by new data from an analysis of the 90 original polished slabs and thin sections, as well as from 20 new thin sections out of Grammer´s samples.

Slope dimensions and slope angles in the Sorbas Basin outcrops based on Terrestrial Lidar data were presented in Reolid et al. (2014). The facies and microfacies based on the data presented in Reolid et al. (2014) are utilized, as well as the additional outcrop description and petrographic analysis of 30 thin sections.
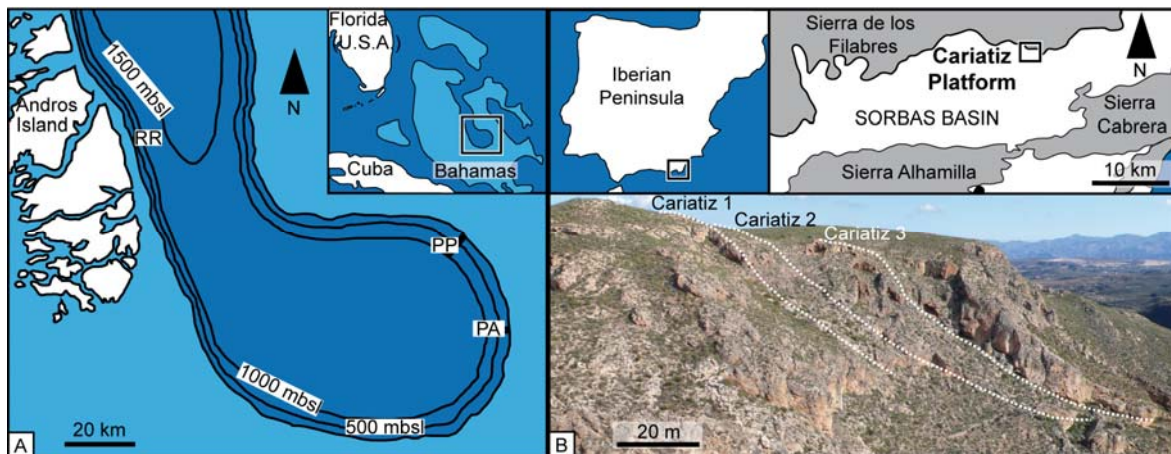
Fig. 4.1: A Location of the Tongue of the Ocean (Bahamas) with slope profiles discussed in the text (RR-Rock Range, PP-Privitt Place, and PA-Palmer Point). **B** Location of the Cariatiz carbonate platform in the Sorbas Basin (Spain). The photography shows the exact location of the outcrops analysed.

4.4 Results

The diverse facies, composition, sedimentary structures, and inclination of the different slopes are documented in Table 4.1.

4.4.1 Tongue of the Ocean slopes

4.4.1.1 Rock Range slope
This 150 m high slope is located along the windward margin of the TOTO. Basinwards, in N70E direction, it extends for nearly 260 m (Fig. 4.2A). The slope can be divided into two

segments with different angles. The upper segment has an inclination ranging from 50° to 60°, followed downslope by a nearly vertical cliff. The lower slope segment is 35° steep.

Slope	Composition	Fabric	Dominant slope facies	Matrix	Microbial features	Dip
Rock Range	US: Red algae, plate-like corals, sponges, and *Halimeda*. MS: *Halimeda*, corals, red algae, molluscs, equinoids, serpulids, bryozoans, and benthic foraminifera. Intraclasts.	US: Wall with cavities and vertical gullies. MS: Poorly bedded with small linear ridges (by submarine sliding).	*Halimeda* floatstone-rudstone.	Microbial micrite. Peloidal micritic matrix.	Microbial micrite including: (1) dense micrite and (2) clotted micrite. Micritic envelops. Trapping and binding structures.	US:50°-60° MS:35°
Privitt Place	US: *Halimeda*, red algae, and sponges. MS-LS: *Halimeda*, red algae, corals, molluscs, benthic foraminifera, and serpulids.	US: Wall with cavities and vertical gullies. MS: 20-30 cm beds. Abundant blocks from US. Slumps. Low relief ridges and swales (by submarine sliding). Cementation. LS: Blocks from US. High relief ridges and swales. Bioturbation.	*Halimeda* floatstone-rudstone (grainstone).	Microbial micrite. Peloidal micritic matrix.	Microbial micrite including: (1) dense micrite and (2) clotted micrite. Micritic envelops. Trapping and binding structures. Microbial domical structures.	US:60°-70° MS:55°-35° LS:32°-30°
Palmer Point	US: *Halimeda*, red algae, and sponges. MS-LS: Peloids. serpulids, corals, ooids, *Halimeda* and molluscs. Minor benthic foraminifera, and bryozoans.	US: Wall with cavities and vertical gullies. MS: 20-30 cm beds. Blocks from US. Low relief ridges and swales (by submarine sliding). Cracks in the slope. Cementation. LS: Poorly bedded. Low and high relief ridges. Bioturbation.	Peloidal packstone-rudstone.	Peloidal micritic matrix. Microbial micrite.	Microbial micrite including: (1) dense micrite and (2) clotted micrite. Micritic envelops. Trapping and binding structures. Microbial domical structures.	US:70°-90° MS:45°-35° LS:30°
Cariatiz 1	US: *Porites* - stromatolite framework and framework blocks (up to 10 m in size). Bivalves, *Halimeda*, echinoids, red algae, brachiopods, and gastropods. Intraclasts.	US: In-situ *Porites* growths. Chaotic breccia. Reef-framework block size decrease basinward.	*Halimeda* breccia and *Halimeda* rudstone.	Microbial micrite. Peloidal micritic matrix.	Reef binding (thick laminated-domical crusts). Microbial micrite including:	US:60° MS:45°-30°
Cariatiz 2	MS: *Halimeda* plates. cm-dm reef-framework blocks. Bivalves (pectinids and oysters), gastropods, serpulids, red algae, echinoid spines, and benthic foraminifera. Intraclasts and minor siliciclastics.	MS: Chaotic. Poorly bedded (beds up to 40 cm thick). Local serpulid-red algal patches up to 1 m wide.	*Halimeda* breccia and *Halimeda* rudstone. Basinal sitls and marls.	Microbial micrite. Silts and marls. Peloidal micritic matrix.	(1) dense micrite and (2) clotted micrite, Micritic envelops binding bioclasts.	US:50°-60° MS:45°-30° LS: 15°-5°
Cariatiz 3	LS: Diatoms. Bivalves (pectinids), gastropods, serpulids, benthic foraminifera, red algae, and echinoid spines. Siliciclastic grains (7-10%).	LS: 5-30 cm thick beds, locally cross laminated. Alternation of slope sediment beds with basinal deposition sediment. Bioturbation.	*Halimeda* breccia and *Halimeda* rudstone. Basinal silts and marls.	Microbial micrite. Peloidal micritic matrix. Silts and marls.	Microbial features absent in LS.	US: 60° MS:40°-30° LS:15°-10°

Table 4.1: Summary of facies and microfacies, type of matrix, microbial features and slope angles at the different segment (upper-US, middel-MS, and lower-LS) of the studied carbonate platform slopes.
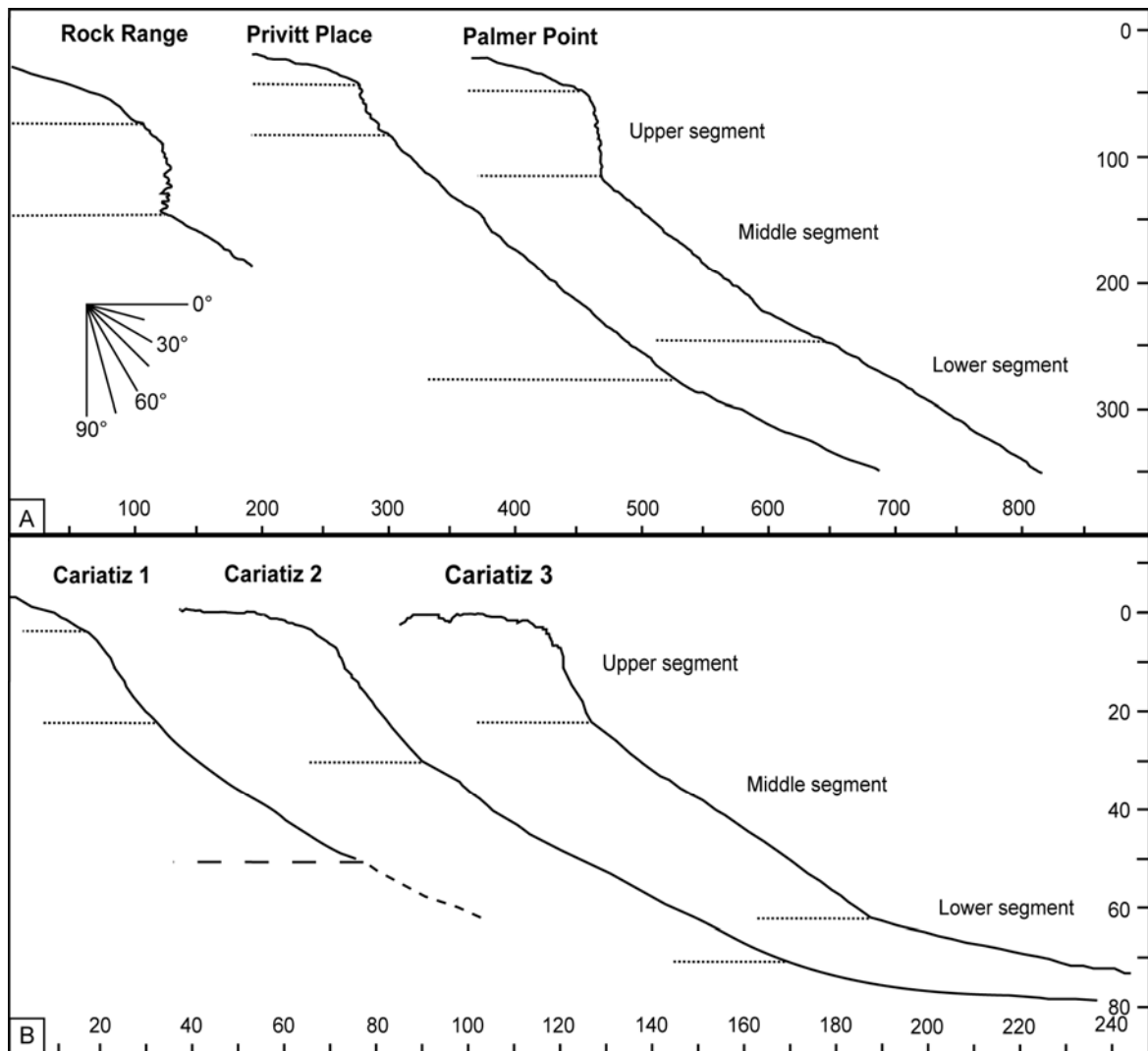
Fig. 4.2: A Tongue of the Ocean slope profiles with different segments (pointed line) with different angles. **B** Cariatiz carbonate platform slope profiles with segments with different angles. Note that the lower slope of Cariatiz 1 is covered. The dashed line indicates the estimated slope gradient.

The uppermost segment of the slope consists of plate-like corals, red algae, sponges, *Halimeda*, and sclerosponges along a ~80 m wall with abundant caves. The floors of these caves are locally covered by recent carbonate mud. The lower segment of the slope is made up of a *Halimeda* floatstone to rudstone with subordinate components such as coral debris, red algae, molluscs, benthic foraminifera, equinoids, serpulids, bryozoans, and intraclasts. Red algae mainly encrust large bioclasts, especially *Halimeda* grains, but also form small nodules. Bioclasts are usually observed floating in a micritic to microgranular matrix that may represent between 30 to 60% of the facies. Up to 85% of the matrix is made of dense to clotted micrite, with minor peloidal micrite. Locally the dense to clotted micrite is distributed in patches connecting bioclasts (Fig. 4.3A) The matrix may locally present a poorly developed layering consisting of an alternation of different packing densities by the binding of silt-sized components in the matrix (Fig. 4.3B). Bladed Mg-

calcite cement occurs lining interparticle and intraparticle voids and locally inside fractures within dense micritic patches (Fig. 4.3C). Botryoidal aragonite cements have a similar distribution in pore spaces but are present exclusively in the coarser grained areas.
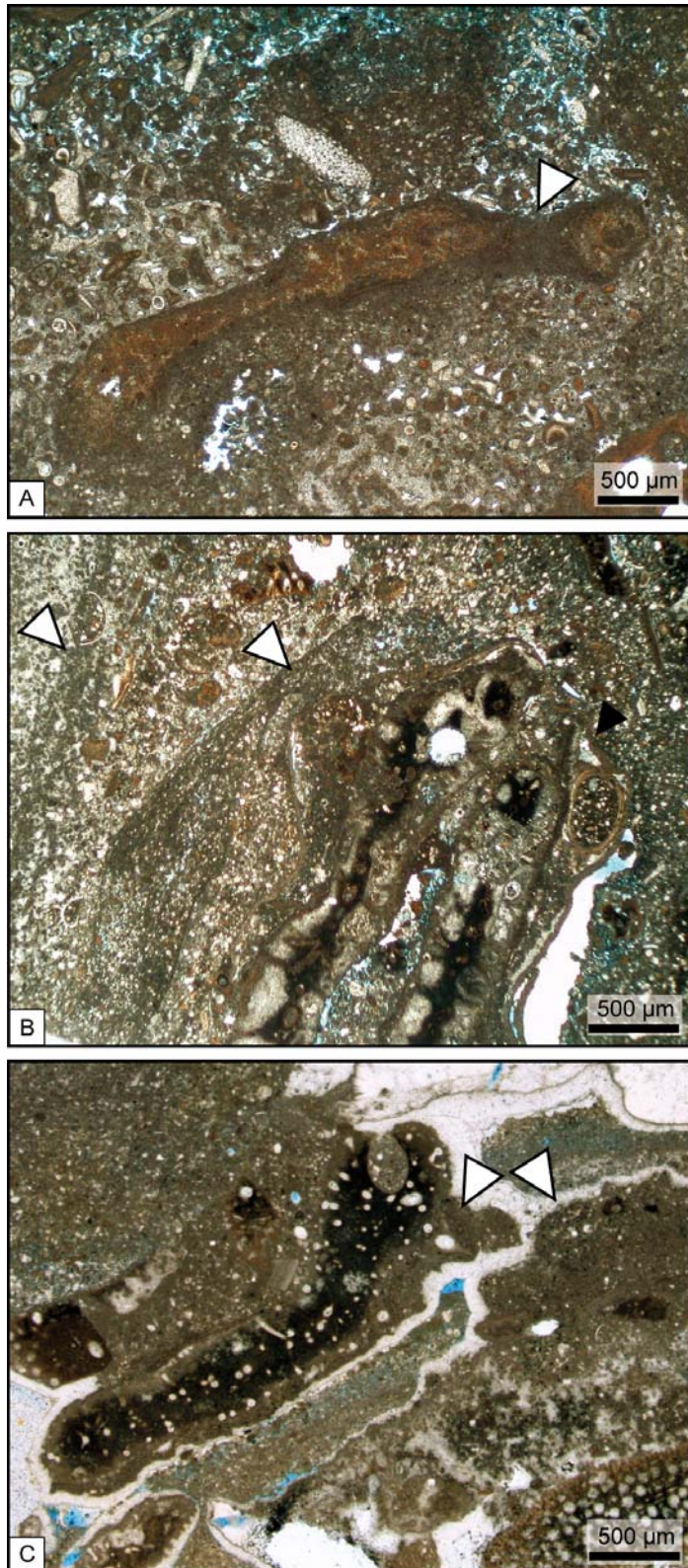
Fig. 4.3: Photomicrographs of the *Halimeda* floatstone from Rock Range slope (TOTO) showing: **A** dense micrite covering and connecting (white arrow) two *Halimeda* plates; **B** alternation of layers (white arrows) defined by different packing density by binding of silt-sized components in the matrix and over two *Halimeda* plates encrusted by red algae (black arrow); and **C** brecciated dense to clotted micrite with calcitic cement infilling the fractures.

4.4.1.2 Privitt Place slope

The 300 m high slope is located on the leeward side of TOTO. Basinwards, in N220E direction, it extends for nearly 540 m (Fig. 4.2A), and has a concave-upward linear profile (sensu Adams and Kenter, 2014), including three segments with different angles. The upper segment comprises angles from 60° to 70°. The middle segment ranges in inclination from 55° in the upper part, to 35° in the lower part. The lower segment has angles between 32° and 30°.

The uppermost segment of the slope consists of a 40 m sub-vertical slope with abundant *Halimeda* as well as red algae and sponges. The middle segment of the slope is characterized by the presence of different sedimentary structures including, from marginal to distal slope parts, large scale slumps and rounded domical structures (moguls), talus slope blocks, and low relief ridges and swales. The rounded domical structures are common around 120 m depth in the middle segment of the slope and are characterized by diameters of 1 to 0.5 m and heights of centimetres to decimetres over the surrounding slope deposits (Fig. 4.4A). These small mounds may exhibit a concentric lamination when broken, suggesting that they may have formed by successive episodes of sedimentation (Fig. 4.4B). The moguls are encrusted by red algae, and the topographic lows among the moguls are occupied by sediment. The sediment in this slope segment consists of *Halimeda* floatstone to rudstone with abundant red algae and coral debris, and minor molluscs, benthic foraminifera, and serpulids. *Halimeda* plates usually contain red algal and micritic crusts (Fig. 4.5A). These micritic crusts may extent over the matrix-binding silt-sized components (Fig. 4.5B). The matrix of this floatstone to rudstone, which comprises up to 60% of the facies, is made of micrite, which locally has a peloidal texture. Micritic peloids are of irregular shape and size. Clotted micrite, locally connecting bioclasts, is the most common texture of the matrix. In some samples the clotted micrite forms up to 80% of the matrix (Fig. 4.6). The clotted micrite eventually occurs partially or totally infilling the primary pores and the interior of some bioclasts. The clotted micrite may retain a porostromate structure (Fig. 4.6) consisting of a concentration of tubular pores. Locally, the micrite is dense and also distributed in patches connecting bioclasts (Fig. 4.7). The facies can be locally described as a grainstone with bladed Mg-calcite and botryoidal aragonite cements. The lower segment of the slope is characterized by the occurrence of high relief (decimetre to metre-scale) ridges and swales. The sediment is similar as in the previously described segment, but shows intense bioturbation with locally minor cementation.

4.4.1.3 Palmer Point slope

This leeward side slope is 290 m high. In N270E direction it extends for nearly 440 m (Fig. 4.2A). The slope has a concave-upward linear profile comprised of three segments

with different inclinations including (1) an upper segment with an inclination ranging from 70° to 90°, (2) a middle segment with angles from 45° in the upper part to 35° in the lower part, and (3) a lower segment with an inclination of 30°.
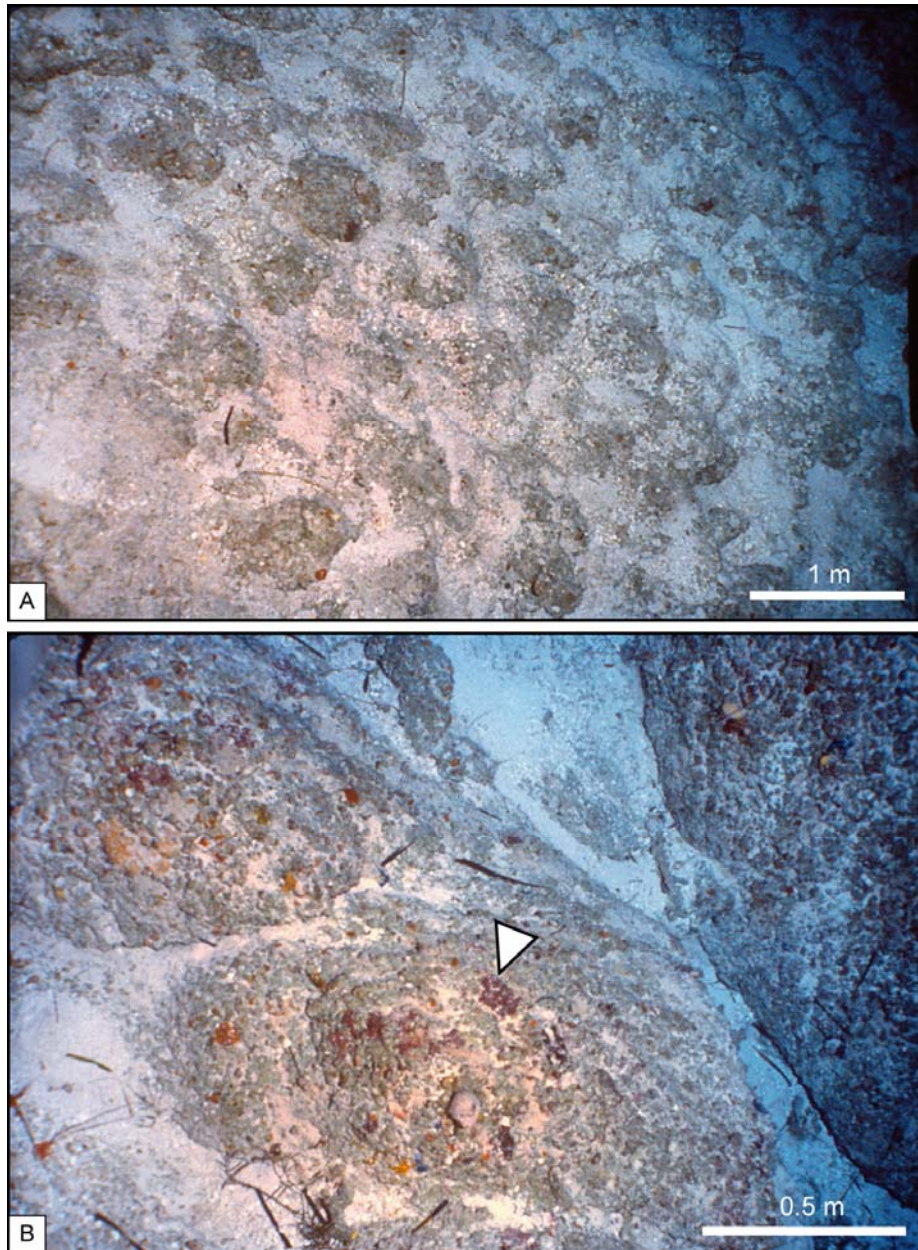
Fig. 4.4: A Photograph taken from the DELTA submersible showing a field of microbial domical structures (moguls) in Palmer Point slope at a water depth of 140 m. **B** Close-up photograph of the microbial domical structures. These structures seem to show an internal concentric lamination and present encrustation by different organism, mainly red algae (white arrow), in the surface.

The uppermost segment of the slope consists of a 70 m wall with caves and vertical gullies. *Halimeda*, red algae, and sponges are the main components in this interval. The middle segment presents moguls in the upper part, around 140 m depth, and some small

low-relief (decimetre scale) ridges that extend basinwards. The moguls, as in the other leeward slope of TOTO (Privitt Place), are a common feature in the uppermost part of the middle segment of the slope with diameters up to 1 m and a height of centimetres to decimetres over the surrounding slope deposits. Red algal crusts may cover the surface of the moguls. The sediment among the moguls consists of a peloidal packstone with abundant serpulids, coral fragments, ooids, *Halimeda* plates, and mollusc fragments. Benthic foraminifera and bryozoans occur as minor components. *Halimeda* plates usually have a micritic crust (Fig. 4.8). The matrix comprises up to a 40% of the facies and consists of micrite, which locally has a peloidal texture. Micritic peloids in the matrix are of irregular shape and size and usually arranged in bands with varying degrees of differential packing (Fig. 4.9). Clotted micrite may be locally present connecting some bioclasts. Bladed Mg-calcite and botryoidal aragonite cements may occur in interparticle and intraparticle voids as well as infilling fractures within dense micritic patches. The lower segment of the slope is characterized by the presence of talus blocks and large (centimetres to metres high and tens of metres long) low-relief ridges and swales. These facies are similar as in the previous segment but shows intense bioturbation and no cementation.
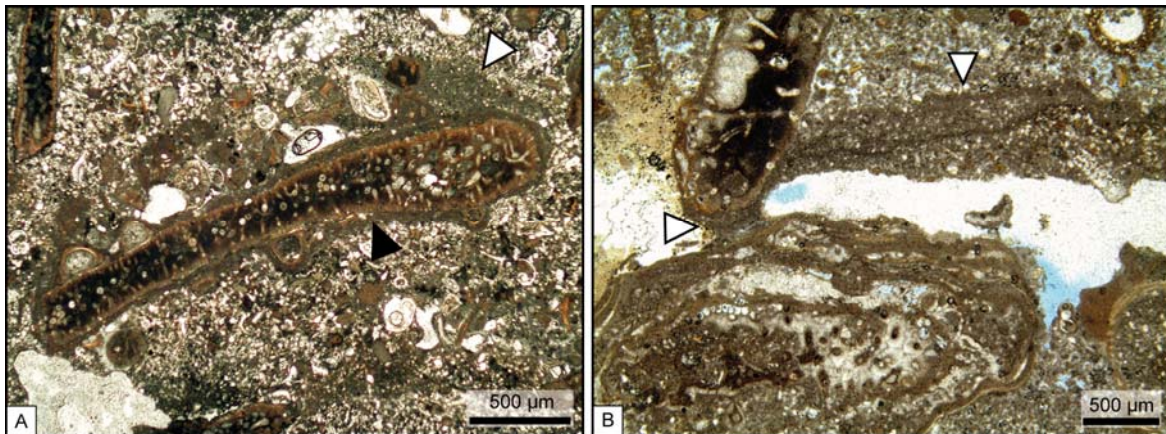
Fig. 4.5: Photomicrographs of *Halimeda* floatstone from Privitt Place slope (TOTO) showing: **A** *Halimeda* plate encrusted by small serpulids, red algae (black arrow) and dense micrite (white arrow); and **B** microbial binding (white arrows) changing into an envelope over a *Halimeda* plate.

4.4.2 Cariatiz slopes

4.4.2.1 Cariatiz slope 1

This clinoform body is 90 m high. The outcropping part of the slope extends for at least 100 m in the direction of progradation (N160E) (Figs. 4.1B, 4.2B). This body has a concave-upward linear to exponential profile, including two segments with different

angles: (1) an upper segment with an inclination of 60°, and (2) a middle segment with angles between 45° and 30°. The lower segment is poorly exposed in the outcrop.

The uppermost part of the body consists of a 7 m thick package of reef framework with *Porites* covered by thin coralline algal-foraminiferal crusts overgrown by thick stromatolitic crusts. A bioclastic matrix fills in the remaining spaces. Downslope there is a 13 m interval characterized by reef-framework blocks. The middle segment consists of a slope breccia comprised of abundant *Halimeda* plates that gradually changes into a bedded *Halimeda* rudstone. Molluscs, serpulids, and rarely red algae occur as minor components. Most of the bioclasts present micritic envelopes locally connecting them (Fig. 4.10A). The matrix represents up to a 60% of the facies and consists of dense micrite, locally with a clotted texture. Micritic peloids are locally common.

Fig. 4.6: Photomicrograph of a sample from Privitt Place slope (TOTO) showing the occurrence of dense and clotted micrite among fine grained bioclasts. The center of the picture (white arrow) displays a concentration of tubular micropores, porostromate structure, separating the micritic clots.

4.4.2.2 Cariatiz slope 2

This clinoform body is 80 m high. In the direction of progradation, it extends for nearly 200 m (Figs. 4.1B, 4.2B). This body has a concave-upward linear profile comprising three segments with different angles. The upper segment has an inclination of 60° to 50°, the

middle segment between 45° and 30°, and the lower segment has angles between 15° and 5°.

The uppermost part of the slope consists of a 15 m thick package of *Porites*-stromatolite reef framework as in the previous slope. Basinward, there is a 25 m interval dominated by reef-framework blocks. The middle segment consists of a slope breccia with *Halimeda*. This facies gradually changes into a bedded *Halimeda* rudstone with molluscs, serpulids, and red algae. Most of the bioclasts present micritic envelopes which locally connect these components. The matrix makes up to 40% of this facies and consists of a dense to layered micrite, which rarely exhibits a peloidal texture. The dense micrite is distributed in patches connecting bioclasts (Fig. 4.7). A poorly developed layering occurs in numerous samples. It consists of an alternation of layers defined by different packing densities of small components and peloids in the matrix (Fig. 4.9). The layering in the matrix can spread over the bioclasts as binding. The lower segment is defined by a change in the degree of lithification, which parallels the basinward decrease in abundance of encrusting organisms. The *Halimeda* rudstones gradually change into bioturbated basinal silts and marls.
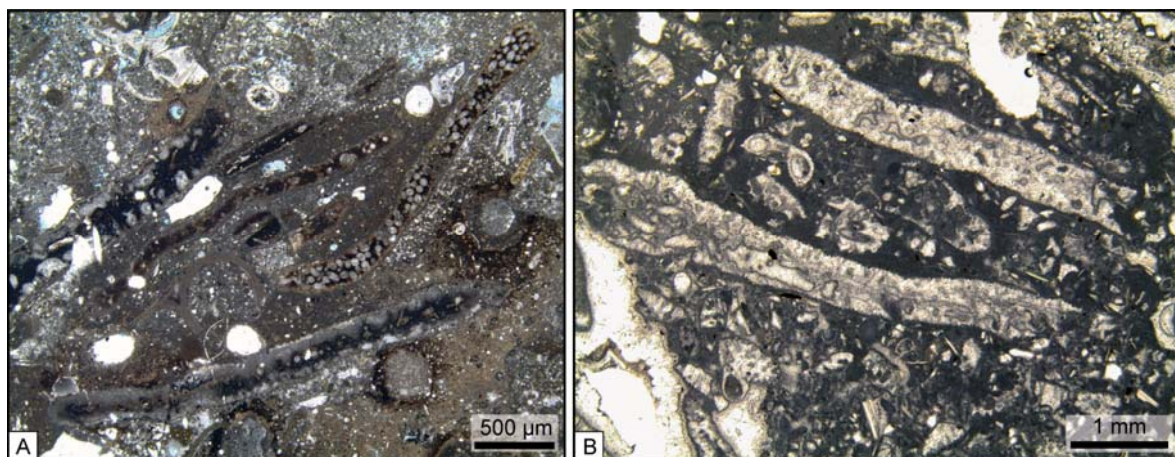
Fig. 4.7: A Photomicrograph of *Halimeda* floatstone to rudstone from Privitt Place (Holocene, TOTO) where dense micrite matrix connects the different *Halimeda* plates. **B** Photomicrograph of *Halimeda* rudstone from Cariatiz slope 1 (Upper Miocene, SE Spain) with dense micrite connecting the different bioclasts. The dense micrite is better developed in the upper part of the bioclasts.

4.4.2.3 Cariatiz slope 3

This clinoform body has a concave-upward linear profile that is 80 m high and extends nearly 200 m in the direction of progradation (CB1 in Reolid et al., 2014) (Figs. 4.1B, 4.2B). The slope has three segments: (1) the upper segment with an inclination of 60°, (2) the middle segment with angles between 40° and 30°, and (3) the lower segment with angles between 15° and 10°.

Fig. 4.8: Photomicrograph of micritic envelopes (white arrows) over *Halimeda* plates from Palmer Point slope (TOTO). The micritic envelopes show different thickness in different sides of the *Halimeda* plates.

The uppermost part of the body consists of a 10 m thick package of *Porites*-stromatolite reef framework. Downslope there is a 22 m interval characterized by reef-framework blocks. The middle segment facies are the breccia with *Halimeda* and the *Halimeda* rudstone. Within the *Halimeda* breccia, some patches of serpulid-tube clusters and red algae occur. Micritic envelopes on the bioclasts are abundant, usually connecting components. The matrix makes up to 50% of the facies and consists of clotted and dense to layered micrite, locally with peloidal texture. Clotted and dense micrite patches, locally connecting bioclasts, are the most common micritic texture in the matrix (Fig. 4.10B). The clotted micrite rarely presents porostromate structure. A poorly developed layering occurs in numerous samples by different packing densities of peloids. Micritic peloids of different sizes are locally abundant. A change in the degree of lithification with decreasing amount of encrusting organisms characterizes the lower segment. The *Halimeda* rudstone gradually changes into bioturbated basinal silts and marls.

4.5 Discussion

4.5.1 Origin of steep slopes

The depositional geometries and the facies distribution in the TOTO slopes, as well as in the Cariatiz carbonate platform slopes, are the response to different sedimentary processes in a fluctuating sea-level context (Grammer and Ginsburg, 1992; Reolid et al., 2014).

65

Rockfalls, gravity flows and in-situ carbonate production were the main processes controlling facies distribution in the upper and middle segments of the studied profiles, while gravity flows and hemipelagic rain, especially at the Cariatiz slopes, were the dominating processes in the lower segments (Grammer and Ginsburg, 1992; Reolid et al., 2014). Grammer et al's. (1993a) observations at the TOTO slopes indicate that windward and leeward slopes present different patterns of Holocene sediment accumulation. The leeward slopes, Privitt Place and Palmer Point, show a significantly better development of the third lower segment of the slope in comparison to the windward slope of Rock Range as a result of greater amounts of sediment being winnowed from the shallow bank top along the open leeward platform (Grammer and Ginsburg, 1992; Grammer et al., 1993a). Schlager (1981) pointed out that the volume of sediment must increase with the platform height to keep the same geometry of the slope, such is the case in the studied outcrops where TOTO slopes are significantly higher than the slopes from Cariatiz according to the greater amount of sediment available in Great Bahama Bank respect to the Cariatiz carbonate platform. However, the slope geometries of both locations are comparable as the volume of sediment in both cases is proportional to the slope size.
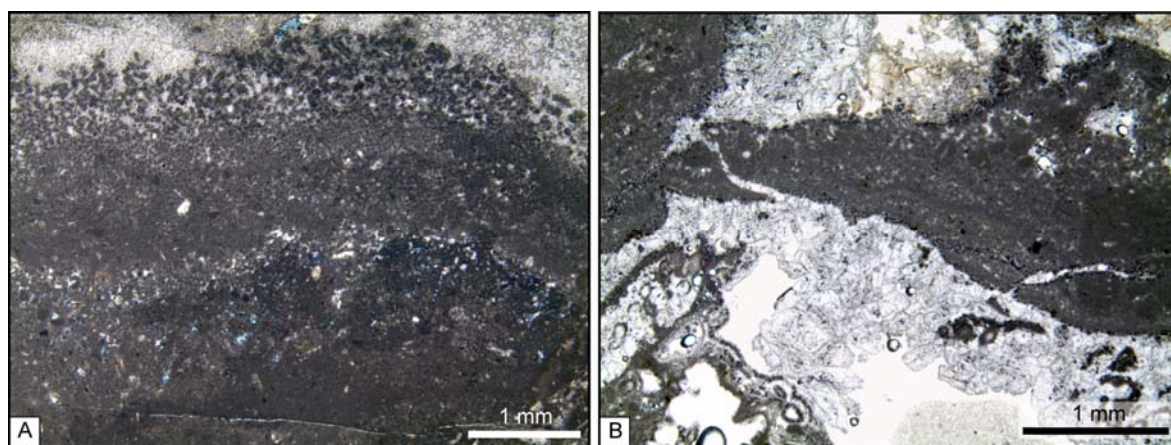
Fig. 4.9: A Photomicrograph of a peloidal micrite showing a differential packing probably related to microbial trapping/binding in Palmer Point (Holocene, TOTO). **B** Photomicrograph of peloidal micrite with microbial binding from Cariatiz slope 2 (Upper Miocene, SE Spain).

The sedimentary processes controlling the facies distribution also shaped the slope profiles. In the upper segment of TOTO profiles, the angles of 60°-90° are interpreted as an erosional cliff developed during the last lowstand (Grammer and Ginsburg, 1992). In the Cariatiz slopes, the imbrication of reef-framework debris at the base of the reef framework allowed the formation of the high angle of 60° in the upper segment (Reolid et al., 2014). The slope angles of 50°-30° in the middle and lower segment of the TOTO slopes and the angles of 45°-30° in the middle segment of the Cariatiz slopes correspond to the maximum angles of repose of sand and gravel (Kirkby, 1987). Although these high

angles of repose are present in these two examples, many other field and seismic examples exhibit lower slope-angles than those described in this work (Fig. 4.11) (Kirkby, 1987; Kenter, 1990; Adams and Schlager, 2000). Together with the grain size, the sediment fabric also exerts a control over the steepness of the slope (Kenter, 1990), however, the slopes studied in both locations are characterized by higher angles than expected for a grain-supported facies (Fig. 4.11).

Steep carbonate slopes, with angles of over 30°-45° (Fig. 4.11), as in the studied profiles, are traditionally described as the result of stabilization by organic framebuilding or early lithification (Kenter, 1990). Processes of early lithification and cementation of the slope sediments, and in-situ carbonate production and stabilization are widely known and reported from Palaeozoic and Triassic examples (Kenter, 1990; Della Porta et al., 2003, 2004; Kenter et al., 2005), but also documented in Neogene slopes from the Gulf of Suez (James et al., 1988), and recently in south Spain (Reolid et al., 2014). In those outcrops, the microbial binding exerts a significant control over the slope geometry favoring the sediment accumulation in high, over 35º, angles of repose (Adams and Kenter, 2014).

In the case of TOTO slopes, Grammer et al. (1993a; 1993b) proposed the rapid growth rate of pore-filling cements as the stabilizing factor of the steep slope angles. According to Grammer et al. (1993a; 1993b) the occurrence of cements in the middle segment of TOTO slopes includes bladed Mg-calcite (infilling approximately up to 31% of the primary porosity), fibrous aragonite (up to a 13%), and botryoidal aragonite (between a 12% and 20%) without any consistent paragenetic trend. Textural evidence suggested that pore-filling botryoidal aragonite cements were one of the last cements to precipitate and AMS radiocarbon dating of botryoidal cements indicate that the cements grew at an average rate of 8-10 mm/100 yr with maximum rates of 25 mm/100 yr (Grammer et al., 1993a). These growth rates and the similarity of radiocarbon ages between some botryoidal cements and coexisting skeletal grains suggest that the majority of cementation took place probably within several tens to a few hundreds of years after deposition of the components (Grammer et al., 1993a).

According to Allen (1985), granular materials first build up to their angle of initial yield, and then undergo shear failure that results in the sediment being left at the more stable angle of repose. Rapid growth rates of pore-filling cements were reported by Grammer et al. (1993a) to favour an extremely rapid cementation and "freezing" of the deposits at their angle of initial yield. However, some of the cements are located in fractures of a previously consolidated, or at least partially consolidated, sediment. This implies that an earlier stage of stabilization preceded cement growth.

4.5.2 Microbial influence on the steep slopes

The presence of an extensive microbial influence in TOTO slopes is proposed as an additional stabilizing factor of the steep slope angles. The microbial coating and binding of the slope sediment would prevent the shear failure of the steep slope deposits and allow the conservation of the original angles of repose for these materials in an early stage (Kenter, 1990; Adams and Kenter, 2014).

A preliminary comparison of TOTO and Cariatiz slopes evidences the similarities in slope geometries and angles, as well as in facies components and microfabrics. In the TOTO slopes, there are distinctive micritic textures considered by some authors as indicative of microbial activity during sediment formation including (1) clotted micrite (Fig. 4.6; Camoin, 1999; Riding, 2000; Reid et al., 2003) with porostromate structures (Fig. 4.6; Andrews, 1986; Lehrmann, 1999; Castagner et al., 2014), (2) dense micrite (Figs. 4.3A, 4.7A; Riding, 2000), and (3) binding structures (Figs. 4.3B, 4.9A; Riding, 2000).
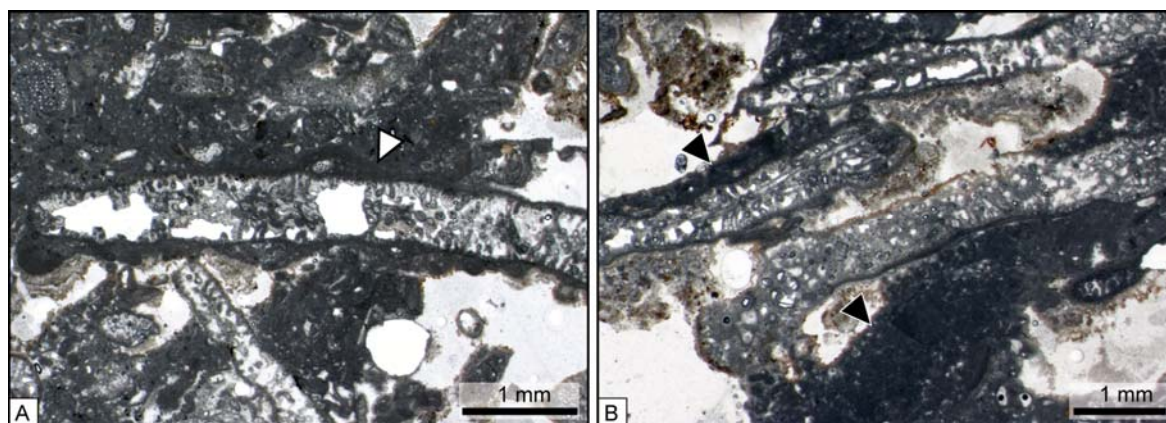
Fig. 4.10: Photomicrographs of the *Halimeda* floatstone to rudstone from the middle segment of the Cariatiz slopes showing: **A** *Halimeda* plate with a micritic envelope that locally preserves the porostromate structure (white arrow); and **B** clotted to dense micrite patches (black arrows) connecting the *Halimeda* plates and preserving the primary interparticle porosity.

The clotted micrite texture (Fig. 4.6), locally connecting bioclasts and partially or totally infilling the primary pores and the interior of some bioclasts, is typically reported as representing microbial agglutination of particles as documented in stromatolites (Reid et al., 2003). The porostromate structure (Fig. 4.6) consisting of a concentration of tubular micropores separating the micritic clots, represents the original morphology of cyanobacteria that mediated the agglutination/precipitation of micrite (Andrews, 1986; Lehrmann, 1999; Castagner et al., 2014). The dense micritic matrix in patches connecting bioclasts (Figs. 4.3A, 4.7A) is also reported as the result of microbial activity by calcification of bacterial cells or biofilms (Riding, 2000).

The interpretation of the dense micrite as calcified biofilms is congruent with the presence of micritic envelopes in some grains, especially on *Halimeda* plates (Figs. 4.3, 4.8). Examples of *Halimeda* accumulations stabilized by organic binding similar to those recorded in TOTO slopes were reported from the Miocene of SE Spain (Braga et al., 1996; Martín et al., 1997). This microbial binding can also be linked to the lamination locally observed in the matrix (Fig. 4.3B) and in banded peloidal aggregates (Fig. 4.9A). Micritic peloids of irregular shape and size, the main component of the facies in Palmer Point slope (Fig. 4.9A), can be also interpreted as calcified microbial aggregates (Riding, 2000).
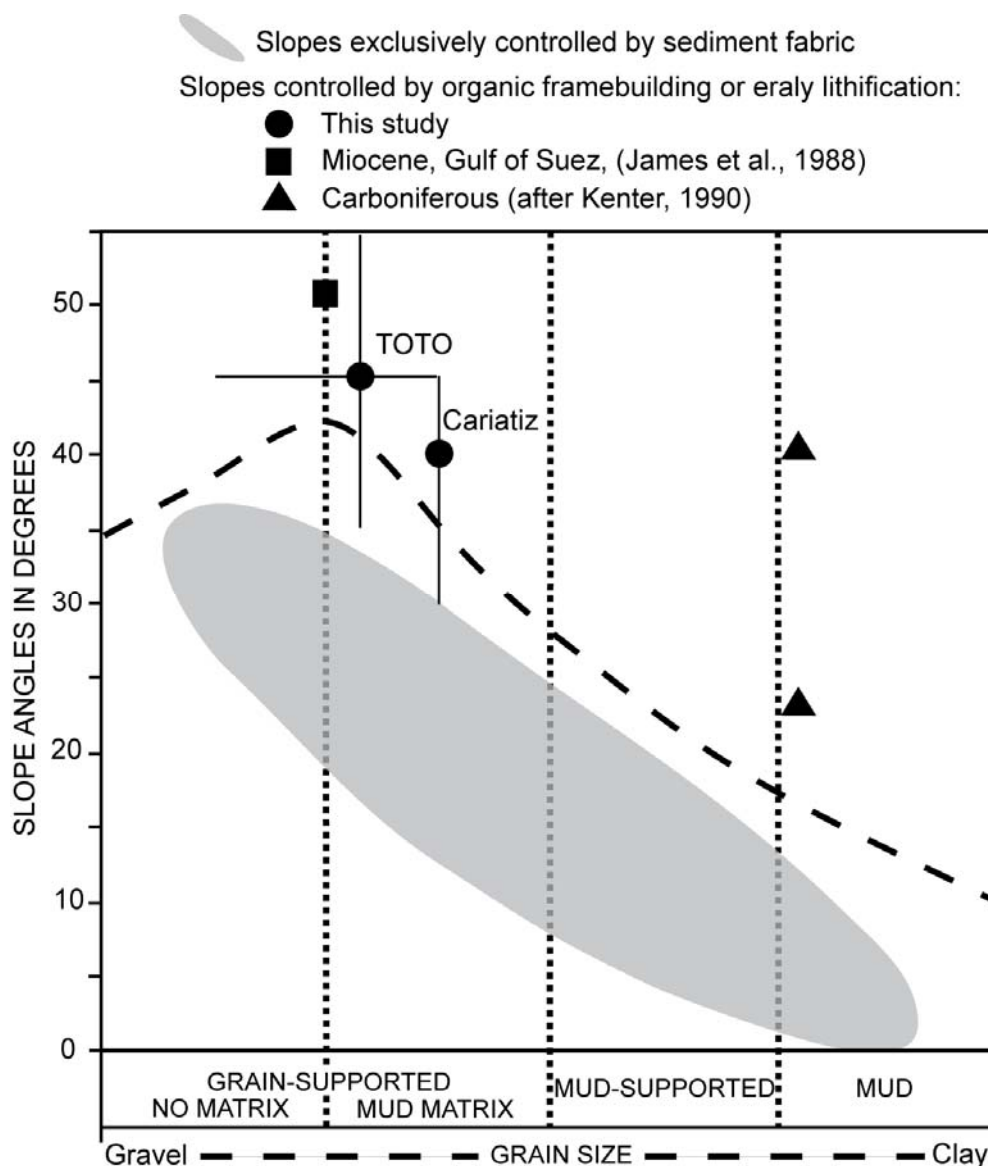
Fig. 4.11: Plot of slope angle vs. dominant sediment fabric (after Kenter, 1990) and vs. grain size (after Kirkby, 1987). The gray field represents the general trend reported from slopes without organic frame building or early cementation. The dashed line represents the maximal angle of repose of sediment ranging in size from gravel to clay. For the slopes presented in this work, the range in slope angle and fabric is indicated by bars.

The moguls in the upper middle segment of the leeward TOTO slopes are another feature of possible microbial origin. Structures similar to the moguls, with diameter of up to 20 cm and diffuse to clear internal lamination, were interpreted as deep water stromatolites formed along foreslopes at depths between 50-100 m below the level of the platform edge in the Gulf of Suez (James, 1988). The microbial stabilization together with the contemporary and later cementation proposed by Grammer et al. (1993a), appear as one process which fosters the preservation of steep slopes in TOTO.

In the Neogene slopes of Cariatiz there are also features reminiscent of microbial activity in distinct facies (Reolid et al., 2014), such as (1) dense micrite among the bioclasts (Fig. 4.7B), (2) micritic envelopes binding the bioclasts (Fig. 10A), (3) clotted micrite connecting the allochems (Fig. 4.10B), and (4) fine peloidal micritic matrix (Fig. 4.9B). The *Halimeda* breccia and *Halimeda* rudstone in the upper and middle segment present the most extensive development of microbial binding, which decreases basinwards as the sediment supply decays and basinal deposition dominates (Reolid et al., 2014).

4.6 Conclusions

This work compares Holocene and Miocene carbonate platform slopes and proposes an explanation for the steep angles of these slopes. The carbonate slopes from the Holocene of the Tongue of the Ocean in the Bahamas and the slopes from an Upper Miocene carbonate platform in SE Spain present slopes with linear profiles and angles in excess of 35°, as well as similar grain sizes, textures and bioclastic components with *Halimeda* plates as a major constituent. The most significant feature of the slope facies is that in the matrix and enveloping bioclasts there are distinctive microfabrics indicative of microbial activity during deposition, such as: (1) clotted micrite patches, locally connecting bioclasts or infilling primary pores, which can present (2) porostromate structure; (3) dense micritic masses; (4) trapping/binding structures; (5) micritic envelopes; and (6) peloidal texture.

The presence of an extensive microbial influence in the studied slopes is proposed as an early-stage slope stabilizing factor, as is the case in Palaeozoic and Triassic carbonate platforms. The occurrence of microbial binding prevented the slope failure in an early stage (several tens of years) and preserved the steep angles of repose of the slope. The occurrence of microbial binding in the Holocene slopes from the Tongue of the Ocean proves that the microbial stabilization in carbonates slopes is significant in normal-marine conditions and not exclusively related to any special conditions such as those of the Mediterranean Sea during the Upper Miocene. This work proves that microbial binding is a previously underestimated factor of slope stabilization in Neogene and Holocene carbonate platform slopes.

References

Adams, E.W., and Kenter, J.A.M. (2014) So different, yet so similar: comparing and contrasting siliciclastic and carbonate slopes. In: *Deposits, Architecture and Controls of Carbonate Margin, Slope and Basinal Settings* (Eds. Verwer, K., Playton, T.E., and Harris, P.M.). *SEPM Special Publication*, 105, 14–25.

Adams, E.W., and Schlager, W. (2000) Basic types of submarine slope curvature. *Journal of Sedimentary Research*, 70, 814–828.

Adams, E.W., Schlager, W., and Wattel, E. (1998) Submarine slopes with an exponential curvature. *Sedimentary Geology*, 117, 135–141.

Adams, E.W., Morsilli, M., Schlager, W., Keim, L., and Van Hoek, T. (2002) Quantifying the geometry and sediment fabric of linear slopes: examples from the Tertiary of Italy (Southern Alps and Gargano Promontory). *Sedimentary Geology*, 154, 11–30.

Adams, E.W., Schröder, S., Grotzinger, J.P., and McCormick, D.S. (2004) Digital reconstruction and stratigraphic evolution of a microbial-dominated, isolated carbonate platform (Terminal Proterozoic, Nama group, Namibia). *Journal of Sedimentary Research*, 74, 479–497.

Allen, J.R.L. (1985) Principles of Physical Sedimentology. George Allen and Unwin, London, 272 pp.

Andrews, J.E. (1986) Microfacies and geochemistry of Middle Jurassic algal limestones from Scotland. *Sedimentology*, 33, 499–520.

Andrews, J.E., Shepard, F.P., and Hurley, R.J. (1970) Great Bahama Canyon. *Bulletin of the Geological Society of America*, 81, 1061–1078.

Berra, F. (2007) Sedimentation in shallow to deep water carbonate environments across a sequence boundary: effects of a fall in sea-level on the evolution of a carbonate system (Ladinian-Carnian, eastern Lombardy, Italy). *Sedimentology*, 54, 721–735.

Bosellini, A. (1984) Progradation geometries of carbonate platforms: examples from the Triassic of the Dolomites, northern Italy. *Sedimentology*, 31, l–24.

Braga, J.C., and Martín, J.M. (1996) Geometries of reef advance in response to relative sea-level changes in a Messinian (uppermost Miocene) fringing reef (Cariatiz Reef, Sorbas Basin, SE Spain). *Sedimentary Geology*, 107, 61–81.

Braga, J.C., Martín, J.M., and Alcalá, B. (1990) Coral reefs in coarse-terrigenous sedimentary environments (Upper Tortonian, Granada Basin, southern Spain). *Sedimentary Geology*, 66, 135–150.

Braga, J.C., Martín, J.M., and Riding, R. (1996) Internal structure of segment reefs: *Halimeda* algal mounds in the Mediterranean Miocene. *Geology*, 24, 35–38.

Braga, J.C., Martín, J.M., and Quesada, C. (2003) Patterns and average rates of late Neogene-Recent uplift of the Betic Cordillera, SE Spain. *Geomorphology*, 50, 3–26.

Camoin, G.F., Gautret, P., Montaggioni, L.F., and Cabioch, G. (1999) Nature and environmental significance of microbialites in Quaternary reefs: the Tahiti paradox. *Sedimentary Geolology*, 126, 271–304.

Castagner, A., Jarochowskab, E., Munneckeb, A., and Desrochersa, A. (2014) Ultrastructures of porostromate microproblematica from a Mulde Event (Homerian, Silurian) bioherm in Podolia, Western Ukraine. *Estonian Journal of Earth Sciences*, 64, 24–30.

Dabrio, C.J., Martín, J.M., and Megías, A.G. (1985) The tectosedimentary evolution of Mio-Pliocene reefs in the province of Almería (SE Spain). In: *Sixth European Regional Meeting of the International Association of Sedimentologists* (Eds. Milá, M.D., and Rosell, J.). *Excursion guidebook*, 269–305.

Della Porta, **G., Kenter, J.A.M., Bahamonde, J.R., Immenhauser, A., and Villa, E.** (2003) Microbial boundstone dominated carbonate slope (Upper Carboniferous, N Spain): microfacies, lithofacies distribution and stratal geometry. *Facies*, 49, 175–208.

Della Porta, G., Kenter, J.A.M., and Bahamonde, J.R. (2004) Depositional facies and stratal geometry of an Upper Carboniferous prograding and aggrading high-relief carbonate platform (Cantabrian Mountains, N Spain). *Sedimentology*, 51, 267–295.

References

Drzewiecki, P.A., and Simó, J.A. (2002) Depositional processes, triggering mechanisms and sediment composition of carbonate gravity flow deposits: examples from the Late Cretaceous of the south-central Pyrenees, Spain. *Sedimentary Geology*, 146, 155–189.

Eberli, G.P., and Ginsburg, R.N. (1989) Cenozoic progradation of northwestern Great Bahama Bank, record of lateral platform growth and sea-level fluctuations. In: *Controls on Carbonate Platform and Basin Development* (Eds. Crevello, P.D., Wilson, J.L., Sarg, J.F., and Read, J.F.). *SEPM Special Publication*, 44, 339 –354.

Enos, P. (1977) Tamabra Limestone of the Poza Rica Trend, Cretaceous, Mexico. In: *Deep-water Carbonate Environments* (Eds. Cook, H.E., and Enos. P). *SEPM Special Publication*, 25, 273–314.

Esteban, M. (1980) Significance of the Upper Miocene coral reefs of the Western Mediterranean. *Palaeogeography, Palaeoclimatology, Palaeoecology*, 29, 169–188.

Esteban, M. (1996) An overview of Miocene reefs from Mediterranean areas: general trends and facies models. In: *Models for Carbonate Stratigraphy from Miocene Reef Complexes of Mediterranean Regions* (Eds. Franseen, E.K., Esteban, M., Ward, W.C., and Rouchy, J.M.). *SEPM Concepts in Sedimentology and Paleontology*, 5, 3–53.

Franseen, E.K., and Goldstein, R.H. (1996) Paleoslope, sea-level and climate controls on upper Miocene platform evolution, Las Negras area, Southeastern Spain. In: *Models for Carbonate Stratigraphy from Miocene Reef Complexes of Mediterranean Regions* (Eds. Franseen, E.K., Esteban, M., Ward, W.C., and Rouchy, J.M.). *SEPM Concepts in Sedimentology and Paleontology*, 5, 159–176.

Franseen, E.K., and Mankiewicz, C. (1991) Depositional sequences and correlation of middle (?) to late Miocene carbonate complexes, Las Negras and Níjar areas, southeastern Spain. *Sedimentology*, 38, 871–898.

Franseen, E.K., Esteban, M., Ward, W.C., and Rouchy, J.M. (1996) Models for Carbonate Stratigraphy from Miocene Reef Complexes of Mediterranean Regions: Introduction. In: *Models for Carbonate Stratigraphy from Miocene Reef Complexes of Mediterranean Regions* (Eds. Franseen, E.K., Esteban, M., Ward, W.C., and Rouchy, J.M.). *SEPM Concepts in Sedimentology and Paleontology*, 5, v–ix.

Ginsburg, R.N. (2001) The Bahamas drilling project: Background and acquisition of cores and logs. In: *Subsurface Geology of a Prograding Carbonate Platform Margin Great Bahama Bank* (Ed. Ginsburg, R.N.). *SEPM Special Publications*, 70, 3–13.

Grammer, G.M. (1991) Formation and evolution of Quaternary carbonate foreslopes, Tongue of the Ocean, Bahamas (unpublished Ph.D. thesis): University of Miami, Rosenstiel School of Marine and Atmospheric Sciences, Miami, 375 pp.

Grammer, G.M., and Ginsburg, R.N. (1992) Highstand vs. lowstand deposition on carbonate platform margins: Insight from Quaternary foreslopes in the Bahamas. *Marine Geology*, 103, 125–136.

Grammer, G.M., Ginsburg, R.N., Swart, P.K., McNeil, D.F., Jull, A.J.T., and Prezbindowski, D.R. (1993a) Rapid growth rates of syndepositional marine aragonite cements in steep marginal slope deposits, Bahamas and Belize. *Journal of Sedimentary Petrology*, 63, 983–989.

Grammer, G.M., Ginsburg, R.N., and Harris, P.M. (1993b) Timing of deposition and failure of steep carbonate slopes in response to a high-amplitude/high-frequency fluctuation in sea level, Tongue of the Ocean, Bahamas. In: *Recent advances and applications of carbonate sequence stratigraphy* (Eds. Loucks, R., and Sarg, R.). *AAPG Memoir*, 57, 107–131.

Haddad, A., Aissaoui, M.D., and Soliman, M.A. (1984) Mixed carbonate-silicic1astic sedimentation on a Miocene fault-block, Gulf of Suez. *Sedimentary Geology*, 37, 182–202.

Halfar, J., and Mutti, M. (2005) Global dominance of coralline red-algal facies: a response to Miocene oceanographic events. *Geology*, 33, 481–484.

Hallock, P., and Schlager, W. (1986) Nutrient excess and the demise of coral reefs and carbonate platforms. *Palaios*, 1, 389–398.

Haq, B.U., Hardenbol, J., and Vail, P.R. (1987) Chronology of fluctuating sea levels since the Triassic (250 million years ago to present). *Science*, 235, 156–167.

Hayward, A.B. (1982) Coral Reefs in a Clastic Sedimentary Environment: Fossil (Miocene, S.W. Turkey) and Modern (Recent, Red Sea). *Coral reefs*, 1, 109–114.

James, N.P., Coniglio, M., Aissaoui, D.M., and Purser, G.H. (1988) Facies and geologic history of an exposed Miocene rift-margin carbonate platform: Gulf of Suez, Egypt. *The American Association of Petroleum Geologists Bulletin*, 72, 555–572.

Kendall, C.G.S.C., and Schlager, W. (1981) Carbonates and relative changes in sea-level. *Marine Geology*, 44, 181–212.

Kenter, J.A.M. (1990) Carbonate platform flanks: Slope angle and sediment fabric. *Sedimentology*, 72, 777–794.

Kenter, J.A.M., Harris, P.M., and Della Porta, G. (2005) Steep microbial boundstone-dominated platform margins - examples and implications. *Sedimentary Geology*, 178, 5–30.

Keim, L., and Schlager, W. (2001) Quantitative compositional analysis of a Triassic carbonate platform (Southern Alps, Italy). *Sedimentary Geology*, 139, 261–283.

Kirkby, M.J. (1987) General models of long-term slope evolution through mass movement. In: *Slope Stability, Geotechnical Engineering and Geomorphology* (Eds. Anderson, M.G., and Richards, K.S.). Jon Wiley and Sons, London, 648 pp.

Krijgsman, W., Hilgen, F.J., Raffi, I., Sierro, F.J., and Wilson, D.S. (1999) Chronology, causes and progression of the Messinian salinity crisis. *Nature*, 400, 652–655.

Land, L.S. (1970) Phreatic versus vadose meteoric diagenesis of limestones: evidences from a fossil water table. *Sedimentology*, 14, 175–185.

Lehrmann, D.J. (1999) Early Triassic calcimicrobial mounds and biostromes of the Nanpanjiang Basin, South China. *Geology*, 27, 357–362.

McIlreath, I.A., and James, N.P. (1978) Facies models 13, Carbonate slopes. *Geoscience Canada*, 5, 189–199.

Mankiewicz, C. (1988) Occurrence and paleocologic significance of *Halimeda* in late Miocene reefs, Southeastern Spain. *Coral Reefs*, 6, 271–279.

Martín, J.M., and Braga, J.C. (1989) Arrecifes Messinienses de Almería. Tipologías de crecimiento, posición estratigráfica y relación con las evaporitas. *Geogaceta*, 7, 66–68.

Martín, J.M., and Braga, J.C. (1994) Messinian events in the Sorbas Basin in the Southeastern Spain and their implications in the recent history of the Mediterranean. *Sedimentary Geology*, 90, 257–268.

Martín, J.M., Braga, J.C., and Rivas, P. (1989) Coral successions in Upper Tortonian reefs in SE Spain. *Lethaia*, 22, 271–286.

Martín, J.M., Braga, J.C., and Riding, R. (1997) Late Miocene *Halimeda* alga-microbial segments reefs in the marginal Mediterranean Sorbas Basin, Spain. *Sedimentology*, 44, 441–456.

Playton, T.E., Janson, X., and Kerans, C. (2010) Carbonate slopes. In: *Facies Models 4, GEOtext 6: Geological Association of Canada* (Eds. James, N.P., and Dalrymple, R.W.). St John's, Newfoundland, 449–476.

Reid, R.P., Dupraz, C., Visscher, P.T., Decho, A.W., and Sumner, D.Y. (2003) Microbial processes forming modern marine stromatolites: microbe-mineral interactions with a three billion-year rock record. In: *Fossil and Recent Biofilms - a Natural History of Life on Earth* (Eds. Krumbein, W., Paterson, D.M., and Zavarzin, G.A.). *Kluwer Academic Publishers*, 103–118.

Reolid, J., Betzler, C., Braga, J.C., Martín, J.M., Lindhorst, S., and Reijmer, J.J.G. (2014) Reef Slope Geometries and Facies Distribution: Controlling Factors (Messinian, SE Spain). *Facies*, 60, 737–753. (Chapter II of this thesis).

Riding, R. (2000) Microbial carbonates: the geological record of calcified bacterial-algal mats and biofilms. *Sedimentology*, 47, 179–214.

Riding, R., Martín, J.M., and Braga, J.C. (1991) Coral stromatolite reef framework, Upper Miocene, Almería, Spain. *Sedimentology*, 38, 799–818.

Schlager, W. (1981) The paradox of drowned reefs and carbonate platforms. *Geological Society of America*, 92, 197–211.

Schlager, W. (2005) Carbonate sedimentology and sequence stratigraphy. In: *Concepts in Sedimentology and Paleontology 8*. SEPM, Tulsa, 200 pp.

Schlager, W., and Camber, O. (1986) Submarine slope angles, drowning unconformities, and self-erosion of limestone escarpments. *Geology*, 14, 762–765.

Schlager, W., and James, N.P. (1978) Low-magnesian calcite limestones forming at the deep-sea floor Tongue of the Ocean, Bahamas. *Sedimentology*, 25, 675–702.

Schlager, W., and Reijmer, J.J.G. (2009) Carbonate platform slopes of the Alpine Triassic and the Neogene - a comparison. *Austrian Journal of Earth Sciences*, 102, 4–14.

Webb, G.E., and Jell, J.S. (1997) Cryptic microbialite in subtidal reef framework and intertidal solution cavities in beachrock, Heron Reef, Great Barrier Reef, Australia: Preliminary observations. In: *Biosedimentology of microbial buildups, International Geological Correlation Programme Project No. 380, Proceedings of 2nd Meeting* Göttingen, Germany (Eds. Neuweiler, F., Reitner, J., and Monty, C.). *Facies*, 36, 219–223.

Willian, C.S., Uchupi, E., Ballard, R.D., and Dettweiler, T.K. (1989) Sea-Floor Observations in the Tongue of the Ocean, Bahamas: An Argo/SeaMARC Survey. *Geo-Marine Letters*, 9, 171–178.